On the Phase Behaviour of the CO2 + N2O4 system at low temperatures

Christophe Coquelet, Esther Neyrolles, Alain Valtz, Antonin Chapoy

On the Phase Behaviour of the CO_2 + N_2O_4 system at low temperatures

Esther Neyrolles[a], Alain Valtz[a], Christophe Coquelet[a,c] and Antonin Chapoy[a,b]

[a] *Mines ParisTech, PSL University, CTP – Centre of thermodynamics of Processes 35 Rue Saint Honoré 77305 Fontainebleau Cedex France*

[b] *Hydrates, Flow Assurance & Phase Equilibria Research Group, Institute of GeoEnergy Engineering, Heriot-Watt University, Edinburgh EH14 4AS, Scotland, U.K.*

c Université de Toulouse, IMT Mines Albi, CNRS UMR 5302, Centre Rapsodee Campus Jarlard, 81013 Albi CT Cedex 9, France

Abstract

Carbon dioxide capture transportation and storage is one of the technologies that can be employed to reduce CO_2 emissions from power plants. Unfortunately, in the post combustion capture process, CO_2 is not pure and contains impurities like SO_2, NO_x, N_2, O_2 and Ar for example. In this paper, Vapour-Liquid-Equilibrium (VLE) of a binary system composed of CO_2 and N_2O_4/NO_2 have been investigated. The equipment used is based on the "static-synthetic" method with a variable cell to determine the bubble pressure or saturated pressure of the system. The setup was used to obtain bubble point data at four isotherms (253.43, 273.43, 293.43, 303.43) K and pressures up to 7.3 MPa. The accuracies of the measured temperature and pressure were estimated to be 0.03 K and 0.12 kPa, respectively. The Peng–Robinson equation of state (PR78 EoS) is used to represent the isothermal *P*, *x* data.

Keywords: Bubble pressure, PVT, Thermodynamic Modelling, Carbon dioxide, Nitrogen Oxides

1. Introduction

To reduce greenhouse gas emissions in the atmosphere, carbon dioxide emissions must decrease as they are mainly responsible for global warming [1]. Most of the CO_2 emissions come from the sectors producing electricity and heat [2]. One of the solutions envisaged to cut emissions is Carbon Capture Utilization and/or Storage (CCUS). It consists of the capture of CO_2 fumes that come out of the combustion plant before their emissions to the atmosphere and to store them underground or reuse them. One of the issues with CCUS is the presence of impurities in the CO_2 fumes, like nitrogen, oxygen, water, sulphur oxides, nitrogen oxides (NO_2, N_2O_4, NO), etc... To be able to treat the fumes correctly, the thermodynamical properties of the CO_2 and N_2O_4 binary system must be known. Another application for this study is the rise of the use of CO_2 as a supercritical green solvent in the chemical industry [3]. For example, for the oxidation of a certain type of cellulose, nitrogen dioxide is used as an oxidant in supercritical CO_2. In the context of the JIP called "Phase Behaviour and Thermophysical Properties of Acid Gases and Related Fluid Systems" started in 2012, Vapour Liquid Equilibrium of several binary systems were investigated (Coquelet et al. [4] and Chapoy et al. [5]). In the paper published by Coquelet et al. [4], it was shown that there is a lack of data concerning binary systems involving NO_2. The only available data on CO_2 and NO_2 binary system are published in the paper by Camy et al. [6]. One reason concerning the fact that there is no VLE data with NO_2 in the context of CCS is that its concentration is very low in fumes. The concentration of NO_2 in the fumes after a combustion plant are at most 400 ppm (mole) according to ISO Technical Report 27921 [7]. Another reason can be the high toxicity of nitrous dioxide. And finally, the chemical analysis of NO_2 is difficult, because nitrous dioxide is reactive. Nitrogen tetraoxide is formed by a monomer dimer association in

the vapour phase from nitrogen dioxide, following the reaction $2\,NO_2 \overset{K_{N2O4}}{\longleftrightarrow} N_2O_4$. Taking into account temperature and pressure, we have examined which species is the predominant one at ambient and low temperature conditions. This reaction occurs in gas phaseand we have assumed ideal gas conditions.

Considering the expression of the chemical potential in the ideal gas condition, the equilibrium constant of this reaction can be expressed following Eq. 1 with P^0 the reference pressure (1 atm in general):

$$K_{N2O4} = \frac{{}^{P_{N_2O_4}}/_{P^0}}{\left({}^{P_{NO_2}}/_{P^0}\right)^2} \quad (1)$$

This equilibrium constant is also called K_p relative to the partial pressures. The equilibrium constant of a reaction is related to its free reaction enthalpy following Eq. 2:

$$K_{N2O4} = e^{\frac{-\Delta_r G^\circ_{association}}{R*T}} \quad (2)$$

The Gibbs free energy of formation of NO_2 and N_2O_4 and the Gibbs free energy of reaction are presented in Table 1.

Table 1: Gibbs free energy of formation of NO_2 and N_2O_4 and Gibbs free energy of reaction of association.

T /K	$\Delta_f G°$ /J.mol^{-1}		$\Delta rG°_{association}$ /J.mol^{-1}
	$NO_{2(g)}$ [a]	$N_2O_{4(g)}$ [b]	
200	45422	68860	-21984
250	48355	83513	-13197
298	51258	97787	-4729
300	51371	98338	-4404
350	54445	113251	4361
400	57560	128204	13084

[a]Data from Chase et al. (1964a) [8]
[b]Data from Chase et al. (1964b) [9]

From the data in Table 1, the equilibrium constant K_{N2O4} can be correlated using Eq. 3:

$$\log_{10}(\mathrm{K}_{N2O4}) = \frac{2982}{\mathrm{T}} - 9.169 \quad (3)$$

The value calculated at 298 K is $\mathrm{K}_{N2O4} = 6.88\, bar^{-1}$. Yoshino et al. [10] have published a value of $\mathrm{K}_{N2O4} = 6.667\ \mathrm{bar}^{-1}$ at 298.54 K considering absorption cross section measurement of NO_2 in the UV and visible region. To evaluate the accuracy of Eq. 1, we have compared our results with literature results. Srivastava and Barua [11] have studied this chemical reaction and published experimental values of dissociation constant of $N_2O_4 \leftrightarrow 2\,NO_2$. Powell and Adams [12] have also published some values of the dissociation constant at 298.15, 308.15 and 413.15 K. Vosper [13] in 1970 has also proposed a temperature dependant correlation for the dissociation constant ($\log_{10}(\mathrm{K}_{dissociation}/atm) = 9.0179 - \frac{2947.4}{\mathrm{T}}$) very similar to Equation 3. Hurtmans et al. [14] have also given a correlation to estimate the dissociation constant ($\log_{10}(\mathrm{K}_{dissociation}/atm) = 22.482 - 0.010469\mathrm{T} + 4.9033 \times 10^{-5}T^2 + 3.2255 \times 10^{-7}T^3 - 4.2181 \times 10^{-10}T^4$). It can be also noted that the reference 1 in Powell and Adams also gives a range of $\mathrm{K}_{\mathrm{dissociation}}$ at 298.15, 308.15 and 318.15 K. K_{N2O4}, varies between 9.039 and 6.865 bar^{-1} at 298.15 K, 3.832 and 3.183 bar^{-1} at 308.15 K and 1.820 and 1.496 bar^{-1} at 318.15 K. Comparisons are shown on Figure 1.

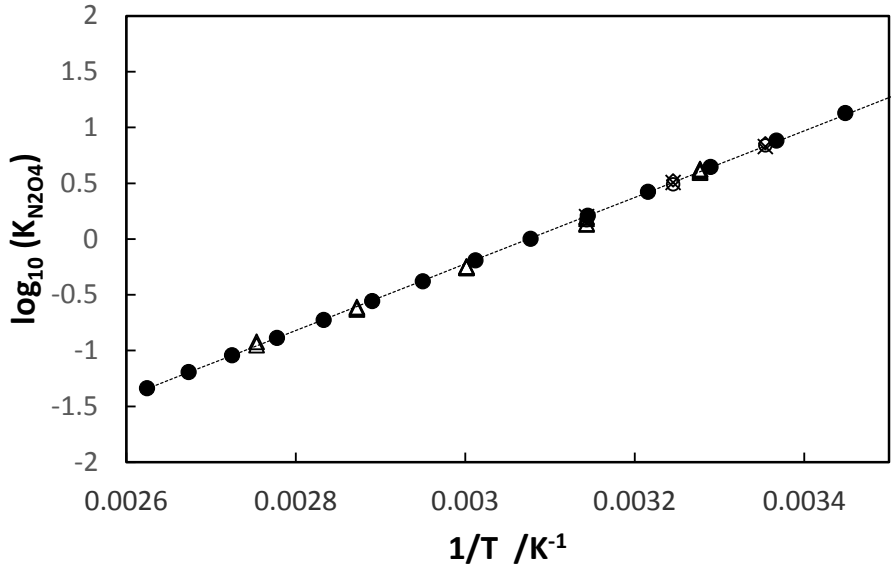

Figure 1: Variation of $\log_{10}(K_{N2O4})$ as a function of inverse of temperature. Dotted line: Equation 1. Symbols (values from literature: (△):Srivastava and Barua [11]**, (×): Reference 2 in Powell and Adams** [12]**, (○): Reference 1 in Powell and Adams** [12]**, (◇):Powell and Adams** [12]**, (●): Calculated values from correlation from Hurtmans et al.** [14]**).**

One important piece of information required for our work is the dissociation fraction. In Table 2, the dissociation fraction of N_2O_4 (x see Table 3), from Pascal and Baud [15] and Pascal [16] are presented at different temperatures. The dissociation fraction of N_2O_4 is expressed following the reaction presented in Table 3.

Table 2: The dissociation fraction of N_2O_4 (x) at different temperatures

T /K	x	x from our equilibrium constant (Eq. 4)	x from Vosper equilibrium constant equation
Pascal and Baud[15]			
299.85	0.1995	0.2005	0.1927
312.95	0.2923	0.3137	0.3008
333.35	0.5284	0.543	0.5222
353.75	0.7991	0.7605	0.7404
373.25	0.8923	0.8893	0.8762
394.65	0.9623	0.9545	0.9479
413.15	1	0.9783	0.9748
Pascal [16]			
313.15	0.2944	0.3157	0.3027
333.15	0.5266	0.5406	0.5199
353.15	0.7589	0.7551	0.7349
363.15	0.9269	0.833	0.816
373.15	0.892	0.8888	0.8757
393.15	0.9588	0.9516	0.9447
413.15	1	0.9783	0.9748

Table 3: Reaction of dissociation of N_2O_4 balance (x is the dissociation fraction)

Reaction:	**N_2O_4** ⟶	**2 NO_2**
t = 0	1	0
t	1 - x	2 x
Partial pressure	$\frac{1-x}{1+x}P$	$\frac{2\,x}{1+x}P$

From Table 3, we obtained Eq 4 (with P°=1 bar).

$$K_{dissociation} = \frac{\left({P_{NO_2}}/{P^0}\right)^2}{{P_{N_2O_4}}/{P^0}} = \frac{4\,x^2}{1-x^2} \times \frac{P}{P^0} \quad (4)$$

To obtain the dissociation fraction, Eq. 4 has to be solved. Considering a total pressure of 1 atm, the dissociation fraction of N_2O_4 was calculated using our equilibrium constant and the one from Vosper. The results are presented in Table 2. An increase of pressure of the reaction [17] works in favour of the production of N_2O_4, or a reduction in pressure shifts the reaction to the production of NO_2. To quantify this affirmation, the dissociation fraction at 298 K is presented as a function of pressure in Figure 22, the data used are estimated from Eq. 4. As can be seen, the dissociation fraction of N_2O_4 is low indicating that the majority compound remains N_2O_4.

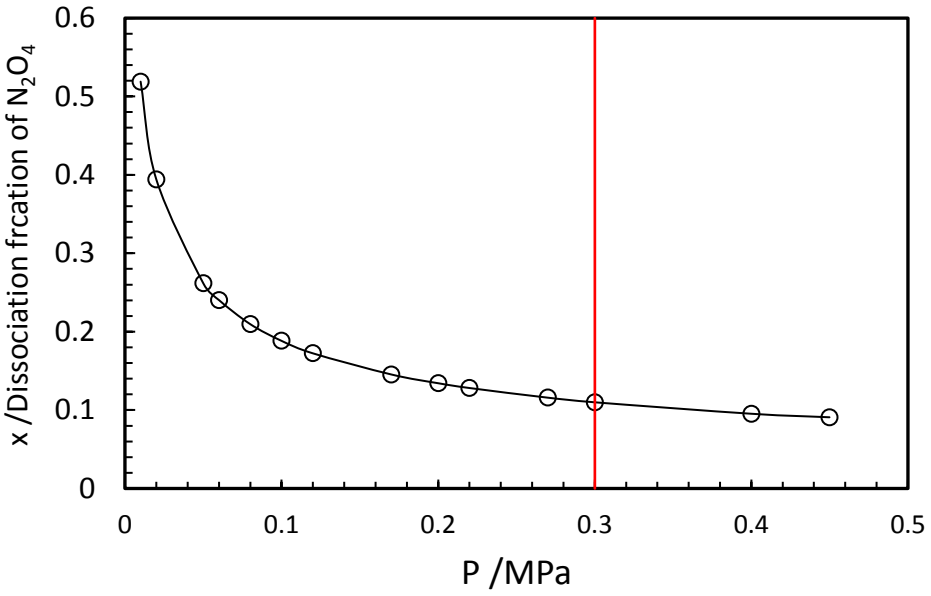

Figure 2: The dissociation fraction of N_2O_4 as a function of the pressure at 298 K estimated from Eq. 4; red curve: minimum pressure of the study

The experimental conditions of our study are high pressure (between 0.3 and 7 MPa) and low temperature (between 217 and 303 K). At these conditions, the ideal gas assumption is not valid and the fugacities have to be included. The dissociation constant can be calculated as:

$$K_{dissociation} = \frac{\left(f_{NO_2}/P^0\right)^2}{f_{N_2O_4}/P^0} = \frac{\left(P_{NO_2}/P^0\right)^2}{P_{N_2O_4}/P^0} \times \frac{\varphi_{NO_2}^2}{\varphi_{N_2O_4}}$$ with φ the fugacity coefficient (lower than 1 when the pressure increase).

Consequently, in comparison to the case where ideal gas state is considered, the reaction will compensate and increase the dissociation fraction of N_2O_4, not so much than that pressure effect which decrease the dissociation fraction. Also, we have considered that only N_2O_4 is present in the liquid and solid phases [18] as the density is very important and it favours the formation of dimer. The analysis previously done also indicates that it will be difficult to quantify the real composition of mixtures composed of CO_2, N_2O_4 and NO_2 due to the association/dissociation reaction, especially using gas chromatography.

Consequently, we have decided to measure the bubble pressure using a "static synthetic" method (i.e. a PVT cell /variable volume cell). The bubble pressure data are correlated with the Peng Robinson Equation of State (PR78 EoS) [19]. For the data analysis of the vapour phase of our experimental data, we have made the approximation that the mixture NO_2-N_2O_4 is always under N_2O_4 form since in our conditions the dissociation fraction seems to be low.

Also, we have estimated by variation of temperature (synthetic-isochoric method) the appearance and disappearance of the solid phase at fixed feed composition. The Solid-Liquid -Vapour (SLV) phase diagram of the binary system is estimated with the same model. Our experimental conditions are from 253 to 303 K for the bubble pressure measurements and at a minimum temperature of 217 K for the SLVE data. The pressure range goes from 0.3 to 7 MPa.

2. Materials and methods

2.1. Materials

The chemicals used in this study are listed in Table 4. No further purification of the chemical products was required.

Table 4: Purities and suppliers of the chemicals used

Chemicals	CAS number	Purity GC[a]	Supplier
CO_2	124-38-9	99.995 vol%	Messer
N_2O_4	10544-72-6	99.95 vol%	Air Liquide

[a] Gas Chromatography

2.2 Experimental set-up

The experiment equipment used was previously presented and described by Coquelet et al. [20] and the schematic diagram of the apparatus is presented in Figure 3.

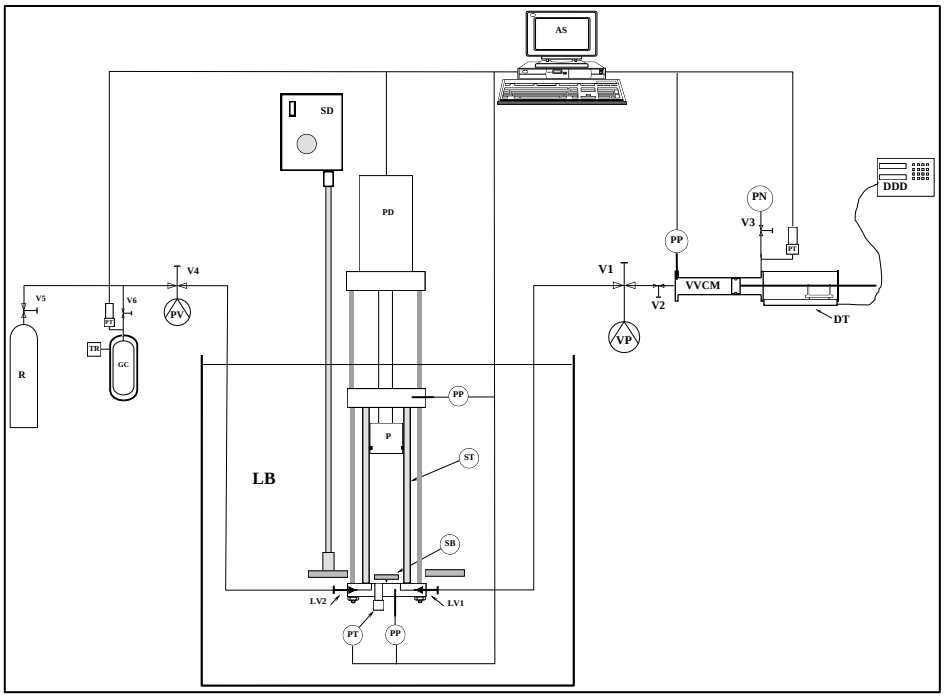

Figure 3: Flow diagram of the apparatus. DAU: Data Acquisition Unit; DDD: Digital Displacement Display; DT: Displacement Transducer; GC: Gas Cylinder; LB: Liquid Bath; LVi: Loading Valve; P: Piston; PD: Piston Monitoring; PN: Pressurized Nitrogen; PP: Platinum Probe; PT: Pressure Transducer; PV (VP): Vacuum Pump; R: Gas Reservoir; SD: Stirring Device; SB: Stirring Bar; ST: Sapphire Tube; TR: Thermal Regulator; Vi: Valve; VVCM: Variable Volume Cell.

A variable volume cell based on a static-synthetic method is used. The equilibrium cell consists of a sapphire tube, held between two titanium flanges with suitable O-rings. The bottom flange contained two valves for loading and cleaning the cell. A magnetic stirrer is installed at the bottom of the cell. The stirring assembly is protected with a suitable corrosion-resistant cover to withstand a corrosive environment. The agitation assembly is magnetically coupled to an external agitation motor, which is capable of producing the desired level of agitation inside the cell. One calibrated 100 Ω platinum resistance thermometer sensor (Pt-100) is used to measure equilibrium temperature at the lower part of the cell. The platinum probe was calibrated by comparison with a 25 Ω reference platinum probe (Tinsley, France). The accuracy of the probe is estimated to be ± 0.03 K. The equilibrium pressure is measured thanks to a cryogenic miniature ruggedized pressure transducer from Kulite® located at the bottom of the cell. A numerical standard (Desgranges & Huot, n° 5202 S CP, France) is used

for the calibration of the pressure transducer at each test temperature. The accuracy was estimated to be ± 12 mbar after calibration. Both temperature and pressure signals from the sensors are transmitted to a computer for the record, via software developed especially for this equipment called PVT Cell Controller. The volume of the cell is modified with a piston. The pressure vs the piston height in the cell is recorded. The display at the breaking point is used to determine the bubble pressure of the mixture. As presented in Figure , the piston is situated at the top of the cell. It is set in motion with a motorized lead screw actuator from Thomson®. A Kollmorgen controller is used to precisely control the downward climb of the piston in the cell. A Tamson TLV 25 thermostatic bath is used to impose and control the temperature of the cell. This bath is equipped with a window to be able to observe the phase change and the descent of the piston during an experiment. A picture of the equipment with a liquid-vapour mixture of N_2O_4 + CO_2 at low temperature is presented in Figure . In this picture, the liquid phase, the gas phase, and the position of the piston in the cell can be seen.

Figure 4: Picture of the cell with the CO_2 + N_2O_4 mixture at low temperature

Each studied mixture is prepared in a variable volume cell, each component is introduced separately and weighed using an Metler Toledo XP2004S mass comparator with an uncertainty of 0.1 mg. The mass composition of the variable volume cell is known by weighting. The variable volume cell is pressurized up to the pressure for the mixture to be

under liquid form and then introduced in the static-synthetic cell. All fractions reported in this paper for L-V equilibrium are in mole fraction. The determination of the bubble pressure is obtained by varying the cell volume. The appearance or disappearance of a gas bubble modifies the compressibility curve (evolution of pressure versus volume). At the break point, i.e. at the change of compressibility curve of liquid/vapour condition and all liquid, it is then possible to determine the bubble pressure.

At equilibrium conditions, each bubble pressure was determined between 2 and 3 times, average values are reported, along with relative standard deviation σ.

3. Results

3.1 Bubble pressure of the CO_2 + N_2O_4 binary system

Bubble point (BP) data of the CO_2 + N_2O_4 system have been measured at 253.43, 273.43, 293.43 and 303.43 K. The results are reported in Table 5 with the associated calculated uncertainties.

Table 5: Experimental and calculated isothermal bubble pressure data for the CO_2 (1) + N_2O_4 (2) mixture system according to the mole fraction of CO_2 x_1 and their standard uncertainties.

T /K		253.43		273.42		293.43		303.43	
x_1	u(x_1)	P /MPa	u(P)	P /MPa	u(P)	P /MPa	u(P)	P /MPa	u(P)
0.254	0.004	0.726	0.005	1.095	0.005	1.608	0.003	1.916	0.006
0.545	0.002	1.165	0.006	1.952	0.000	3.026	0.002	3.685	0.001
0.716	0.004	1.469	0.002	2.490	0.003	3.891	0.004	4.741	0.004
0.833	0.003	1.756	0.010	2.925	0.008	4.622	0.013	5.659	0.013
0.942	0.005	1.872	0.004	3.274	0.002	5.274	0.006	6.518	0.007
1	0.00002	1.997	0.001	3.519	0.009	5.751	0.007	7.301	0.012

Expanded uncertainties (k = 2) U(T) = 0.03 K

The experimental bubble points of the system were correlated using the Peng Robinson equation of state (PR78 EoS) Eq. 5 [19] with the Mathias-Copeman alpha function (Eq. 6) [21] and the classical van der Waals mixing rules (Eq. 7).

$$P = \frac{RT}{v-b} - \frac{a}{v(v+b)+b(v-b)} \tag{5}$$

With $a = a_C \alpha(T_R, \omega)$; and $a_{Ci} = 0.45724 \frac{R^2 T_{Ci}^2}{P_{Ci}}$, $b_i = 0.07780 \frac{RT_{Ci}}{P_{Ci}}$

$$\alpha(T) = \left[1 + c_1\left(1 - \sqrt{\frac{T}{T_C}}\right) + c_2\left(1 - \sqrt{\frac{T}{T_C}}\right)^2 + c_3\left(1 - \sqrt{\frac{T}{T_C}}\right)^3\right]^2 \tag{6}$$

$$a = \sum_i \sum_j z_i z_j a_{ij} \text{ , with } a_{ij} = \sqrt{a_i a_j}\left(1 - k_{ij}\right) \text{ and } b = \sum_i z_i b_i \tag{7}$$

The properties of each component are reported in Table 6**.**

Table 6: Properties of CO_2 and N_2O_4 pure components[a]

Compound	T_c /K	P_c /MPa	MC			ω	T_m /K	P_t /MPa	$\Delta H_{S \rightarrow L}$ /J.mol^{-1}
			C_1	C_2	C_3				
CO_2	304.13	7.373	0.7138	-0.4422	2.4364	0.224	216.58	0.518	8652.3
N_2O_4	431.4	10.1	2.0690	-3.7228	3.1108	0.834	261.85	0.019	14650

[a]Data from DIPPR 801 database

The parameters of the Mathias-Copeman alpha function were adjusted to experimental vapour pressure of N_2O_4 using several literature data: Scheffer and Treub [22], Egerton [23], Smith [24] and Giauque and Kemp [25]. The adjusted parameters are found in Table 6 and the deviations (Bias and Absolute Average Deviations AAD) are presented in Table 7. The vapour pressure calculations obtained with the PR 78 EoS and the original alpha function are also compared in Table 7. As seen in Figure 5, the PR78 EoS combined with the Mathias-Copeman alpha function can reproduce the literature experimental vapour pressure from the triple point to the critical point.

Table 7: Deviations between experimental and calculated vapour pressures

	Bias/%		AAD/%	
Alpha Function	**Mathias Copeman**	**Classical**	**Mathias Copeman**	**Classical**
All data	-0.02	-0.5	1.0	12
Scheffer and Treub [22]	-0.6	-15	0.9	15
Baume and Robert [26]	-0.8	5.2	1.1	9.7
Mittasch et al. [27]	0.02	-2.4	0.4	9.9
Tsymarnyi [28]	-0.8	-10	1.1	10
Smith [24]	0.8	13	1.6	13
Stoddart [29]	2.9	17	3.4	17
Scheffer and Treub [30]	-1.0	5.0	1.0	12

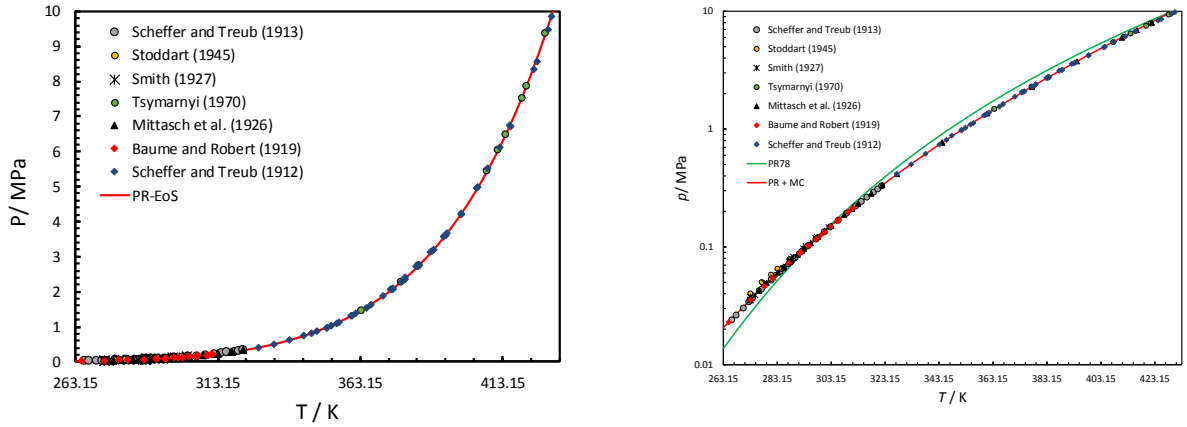

Figure 5: Vapour pressure of N_2O_4 as a function of the temperature from 261.9 to 430 K, ◆: data from [22]; ◆: data from [26]; ▲: data from [27]; ●: data from [28]; ✳: data from [24]; ●: data from [29]; ●: data from [30]; red line: calculated with PR78 EoS. Green line: Calculated with PR78 EoS with the original alpha function.

The experimental and modelling results for each different isothermal condition are plotted in Figure 6.

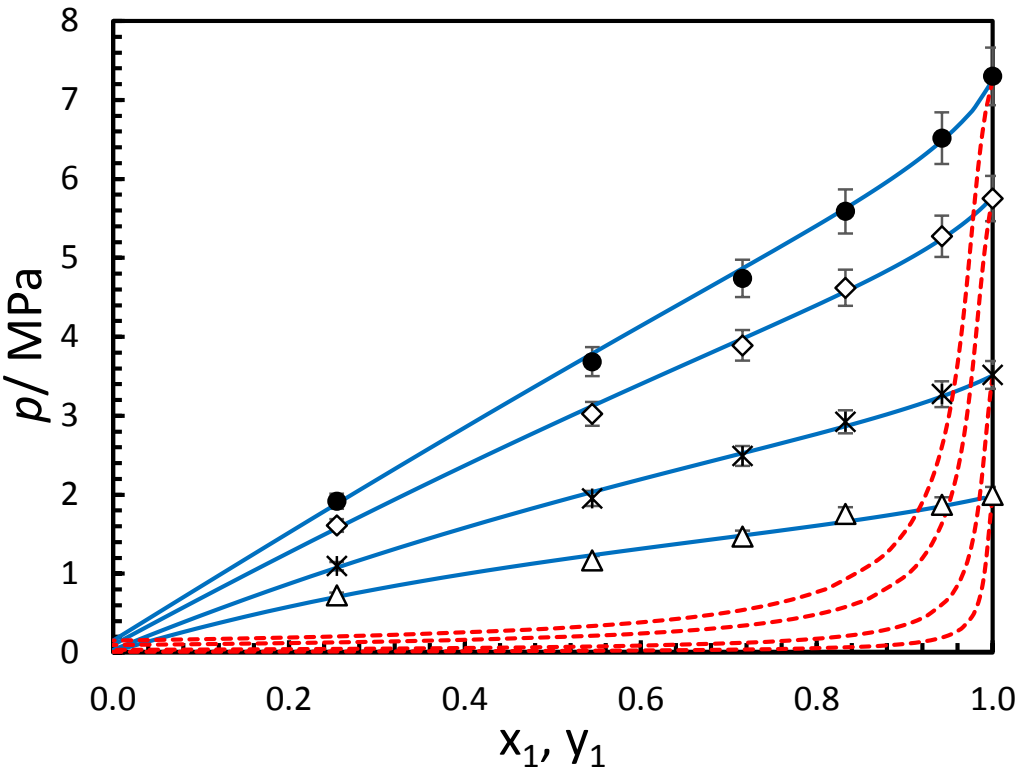

Figure 6: Bubble point of the CO_2 (1) + N_2O_4 (2) binary system as a function of the CO_2 (1) mole fraction between 253 and 303 K. △: 253.43 K; ∗: 273.43 K; ◇: 293.43 K; ●: 303 K; Full line: bubble point calculated with the PR78 and k_{ij} from Eq. 9. Dashed line: dew point calculated with the PR78 and k_{ij} from Eq. 9.

The binary interaction parameters between carbon dioxide and Nitrogen tetraoxide were adjusted directly to VLE data through a modified Simplex algorithm using an objective function based on bubble pressure calculations given in Eq. 8.

$$F = \frac{100}{N}\left[\sum_1^N \left(P_{\text{exp}} - P_{\text{cal}}\right)^2\right] \quad (8)$$

The values of the adjusted binary interaction parameter, k_{ij}, for each individual experimental isotherm are plotted in Figure 7 and listed in Table 8. The binary interaction parameters, k_{ij}, can be correlated as a function of the temperature using the following Eq. 9.

$$k_{ij} = 4.8282 \times 10^{-6}\, T^2 - 3.2244 \times 10^{-3} T + 4.6345 \times 10^{-1} \quad (9)$$

Table 9 presents the AAD (Average Absolute Deviation) and Bias on bubble pressure calculation, estimated from, respectively, Eqs. 10 and 11. In Table 9 the deviations between the model and the data from Camy et al. [6] are also presented.

$$AAD = \frac{100}{N} \sum \left| \frac{P_{\text{cal}} - P_{\text{exp}}}{P_{\text{exp}}} \right| \quad (10)$$

$$\text{Bias} = \frac{100}{N} \sum \frac{P_{\text{exp}} - P_{\text{cal}}}{P_{\text{exp}}} \quad (11)$$

Table 8: k_{ij} parameter and F function

T /K	k_{ij}	F
253.43	-0.043	0.299
273.42	-0.058	0.245
293.43	-0.067	0.452
303.43	-0.071	0.624
ALL T	-0.064	0.808

Table 9: Deviations in Pressure using the Peng Robinson Equation of State with the Mathias Copeman Alpha function and the classical mixing rules.

	T /K	*BIASP* /%	*AADP* /%
Camy and al. [6]	298.15	7.90	7.90
	313	3.18	5.70
	328.45	-3.65	3.65
	All T	2.25	5.46
This work	253.43	-0.36	3.14
	273.42	0.14	2.04
	293.43	0.23	1.86
	303.43	0.46	1.66
	All T	0.12	2.17

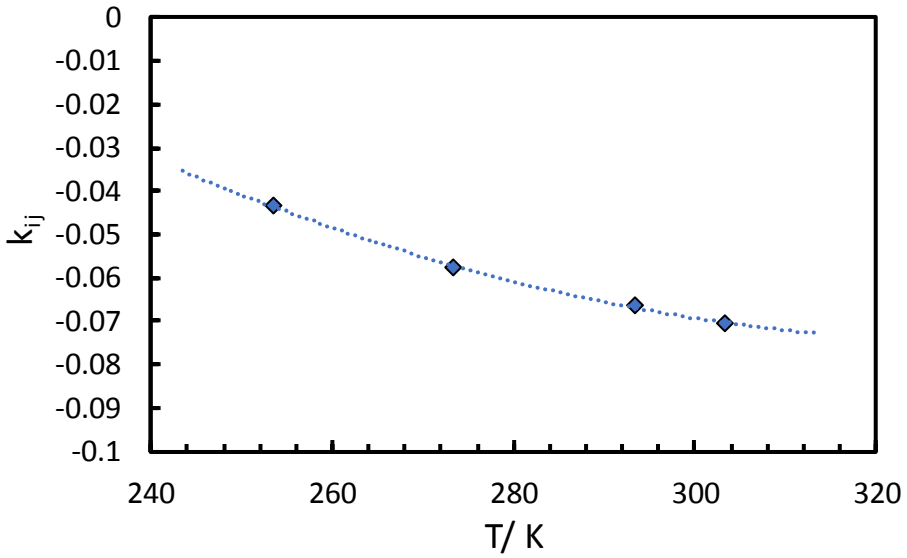

Figure 7: k_{ij} parameter as a function of the temperature

The only available literature data for comparison are from Camy et al. [6]. They have studied this binary system using a similar experimental technique. The data are presented in Figure 8 and are predicted with the PR78 EoS with k_{ji} estimated from Eq. 9.

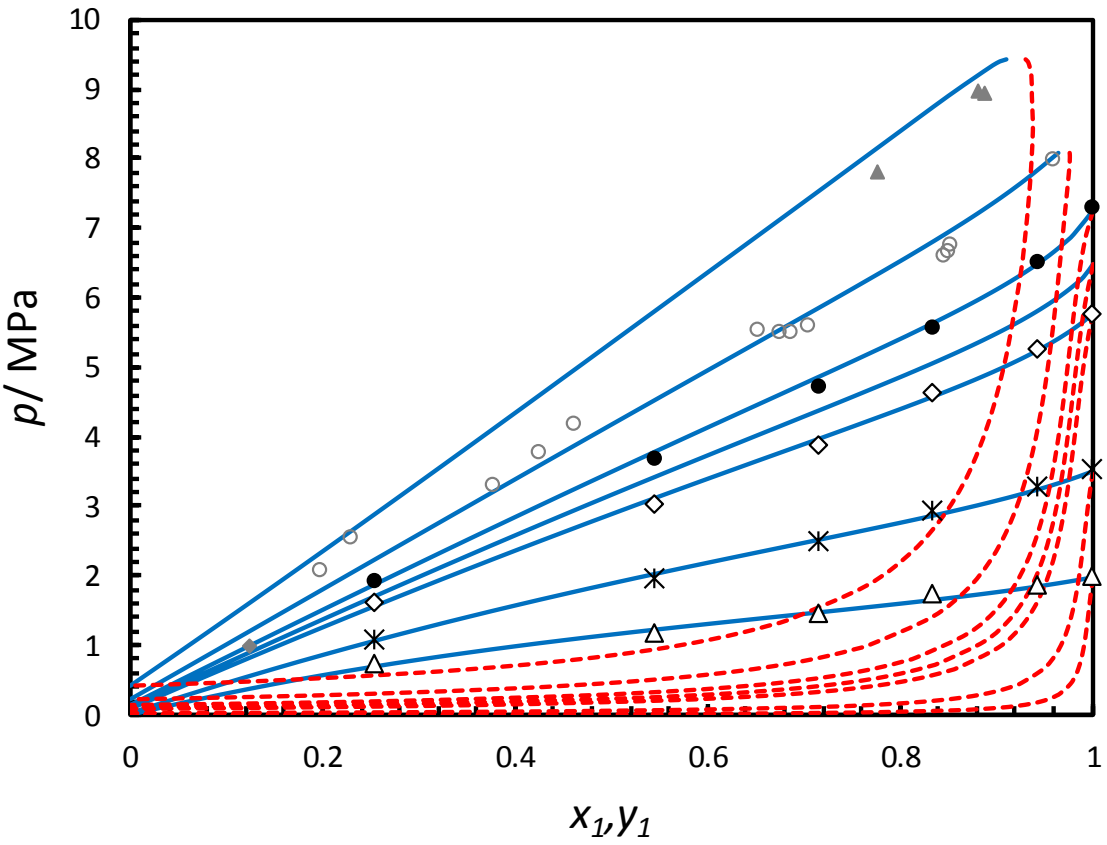

Figure 8: Bubble point of the CO_2 + N_2O_4 binary system as a function of the CO_2 (1) mole fraction between 253 and 303 K. Experimental data from Camy et al. [6]: ◆: 298 K; ○: 313 K; △: 323 K; Dashed line: calculated from PR78 EoS with k_{ij} calculated using Eq. 9.

As seen from Figure 8, a fair agreement between our work and the literature data can be observed. We can also note that the data of Camy et al. [6] are showing larger scattering.

3.2 Solid-Liquid-Vapour (SLV) study of the CO_2 + N_2O_4 binary system

For each composition of the CO_2 + N_2O_4 mixture studied, the temperature of appearance and disappearance of a solid phase was experimentally determined. Considering the melting temperatures (Table 5) of each component, considerate is assumed that solid phase is mainly composed of N_2O_4. The temperature of the system was decreased until the solidification was noticeable to the eye, as presented in Figure 9. This decrease in temperature was stepwise.

Then the temperature was increased stepwise until the N_2O_4 solid disappeared. Those steps were repeated several times until the temperatures between freezing and melting were around 2 K apart.

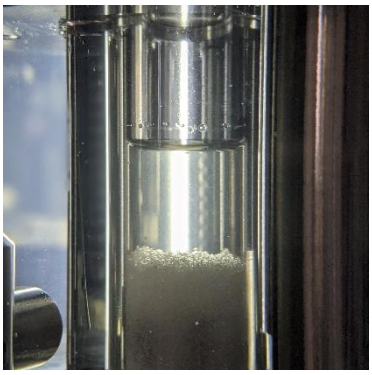

Figure 9: Picture of the cell with SLV of the CO_2 + N_2O_4 mixture.

With this experimental apparatus, the lowest achievable temperature is around 213 K, so we only determine the melting point above this temperature. The experiments were conducted for three different compositions. The results are presented in Table 9.

Table 10: Experimental melting point data on the CO_2 (1) + N_2O_4 (2) at three mole fraction in CO_2 x_1 binary system

T_m (K)	x_1	$u(x_1)$	P /MPa
249.83	0.254	0.004	0.56
230.15	0.545	0.002	0.53
217.05	0.716	0.004	0.44

Expanded uncertainties (k = 2) u(T) = 2 K, u(P) = 0.002 MPa

The chosen approach for modelling the Solid-Liquid (SL) phase diagram of the CO_2 + N_2O_4 binary system, is the fugacity (f^i) equality, following Eq. 10. It is assumed that the solid phases stay pure.

$$f_S^i = f_L^i \tag{10}$$

The fugacity of the solid phase can be estimated, with Eq. 11, according to Prausnitz et al. [31]:

$$f_S^i = f_L^* \times e^{\left(\frac{\Delta H_{S\to L}}{RT}\times\left(\frac{T}{T_m}-1\right)\right)} \quad (11)$$

With f^*_L: the fugacity of the pure compound, $\Delta H_{S\to L}$: the melting enthalpy, T_m: temperature of the melting point (see Table 6).

The experimental SLV measurements were calculated using PR-EoS and the binary interaction parameters tuned on VLE measurements (Eq 9). The predictions of the model are in fair agreement with the measured melting points. As seen in Figure 10, the PR78 EoS estimations are in relatively fair agreement at 250 K, but they deviate from the experimental values at lower temperatures. This mixture is predicted to present an eutectic point with a molar composition in CO_2 close of 0.8 (0.68 mas fraction) with a temperature close to 208 K.

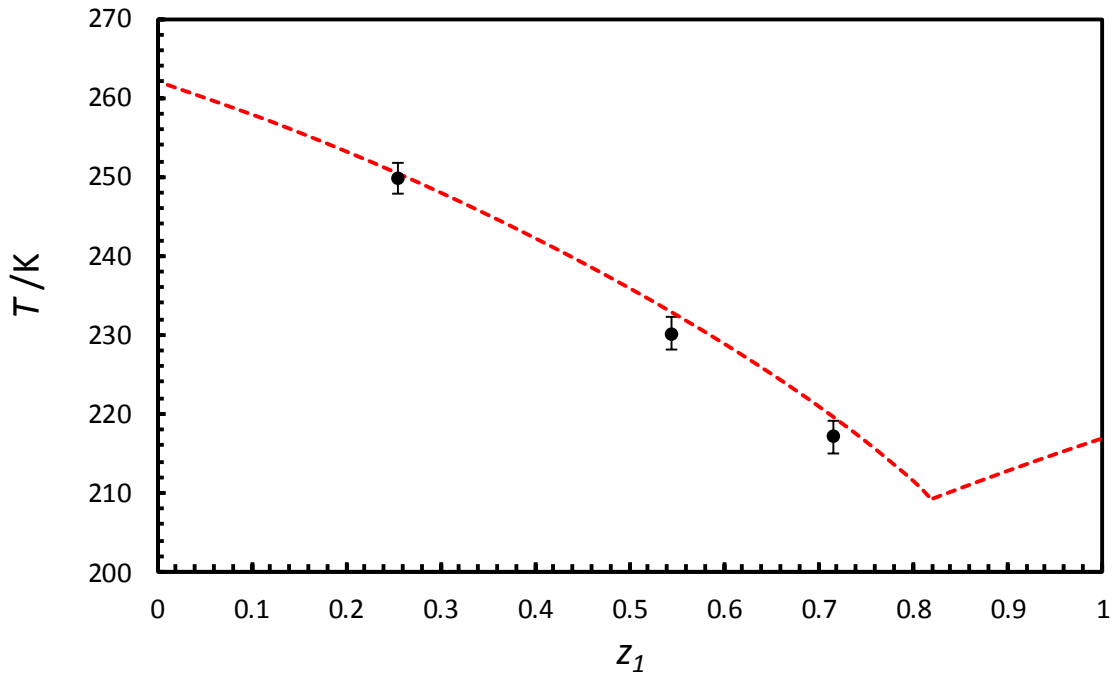

Figure 10: Melting temperature as a function of the CO_2 mol fraction; ●: experimental data; dashed line: calculation based on fugacity estimated from N_2O_4 as pure solid phase with k_{ij} from Eq. 8; dotted line: calculation based on fugacity estimated from CO_2 as pure solid phase with k_{ij} from Eq. 8

Additional measurements are required to have a better characterisation of the region close to the eutectic point.

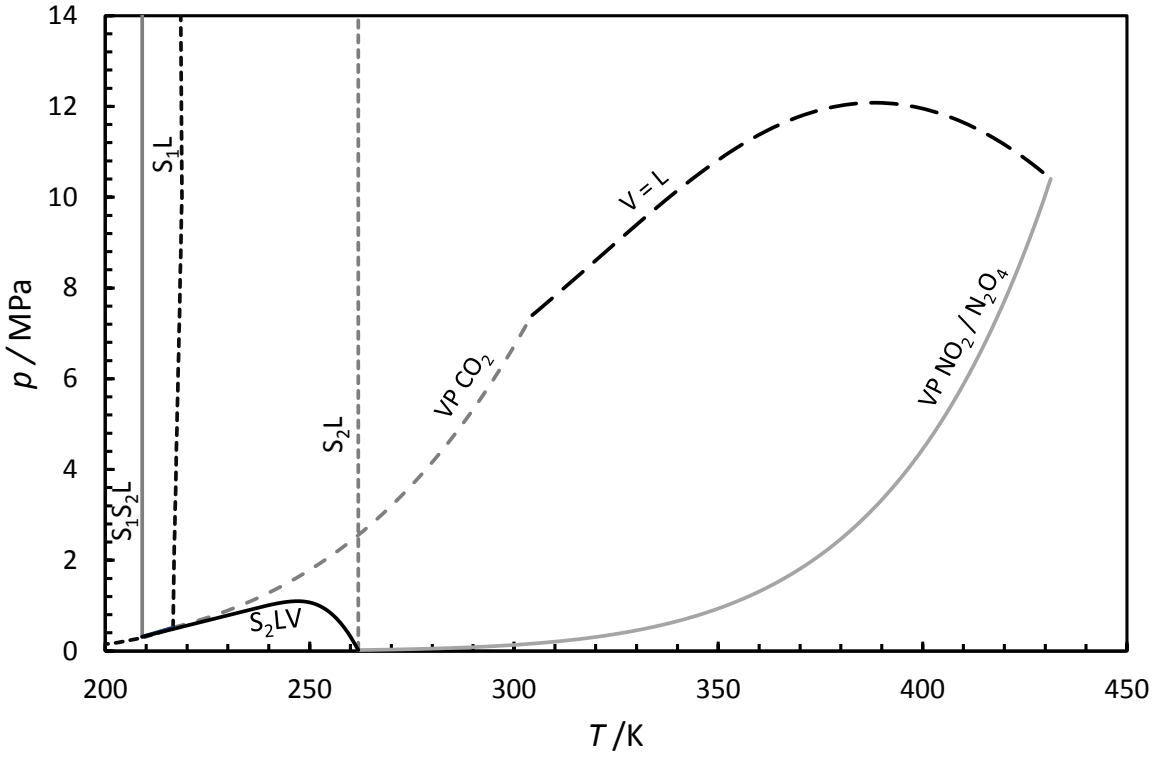

Figure 11: Pressure–temperature equilibrium behaviour for the CO_2 – N_2O_4 system (S_1: solid CO_2; S_2: solid N_2O_4; VP: vapour pressure; V=L: vapour–liquid critical locus).

The pressure – temperature equilibrium behaviour of the CO_2 + N_2O_4 binary system is qualitatively illustrated in Figure 11. The thermodynamic model considered in this paper did not allow for a complete description of the actual behaviour of the system, *i.e.*, the dissociation degree of N_2O_4 was not measured. In 2008, Belkadi et al. [32] have applied the crossover soft-Saft model to describe the CO_2+NO_2/N_2O_4 system. The authors have considered NO_2 has a self-associating molecule. The authors have shown that the NO_2 is a strong associating fluid and a relatively good agreement was observed with the data from Camy et al. but with values of deviation increasing with the pressure and the temperature. With this model, they have shown that the liquid phase is mainly composed of N_2O_4 at low temperature (T<300K). An alternative method would be to use the approach developed by Anderko [33]. The author has considered the chemical theory approach where the compressibility factor is the sum of two contribution (physical and chemical) $Z = Z^{ph} +$

$Z^{ch} - 1$. The Peng Robinson Eos can be considered to calculate the physical part of the compressibility factor. For the chemical part, the Mecke-Kempter assumption (Eq. 12 with P^0 the standard pressure 0.101 MPa, v the molar volume and K the equilibrium constant) can be considered with the equilibrium constant given by Eq. 3.

$$Z^{ch} = \frac{2}{1+\sqrt{1+(4RTK/P^0 v)}} \quad (12)$$

Using all the new data presented in this paper, such a model can be developed.

4. Conclusion

The bubble pressures of the CO_2 + N_2O_4 binary system were experimentally measured between 253 and 303 K using a static-synthetic apparatus. The new data were compared to literature data and good agreement was found. Binary interaction parameters k_{ij} of PR78 EoS were adjusted assuming that only nitrogen tetraoxide was present in the liquid phase, and a temperature dependency of the k_{ij} was found. The same equipment was also used to measure the melting temperature of three mixtures rich in N_2O_4. Based on our experimental data, it appears that the binary system presents a eutectic point. However, further measurements are required for a final validation.

5. Acknowledgments

This work was a part of the JIP project "Impact of Common Impurities on Carbon Dioxide Capture, Transport and Storage" which the phase-III was conducted jointly at Heriot-Watt University in Edinburgh, UK and MINES ParisTech in France in 2017–2021. The authors would like to gratefully acknowledge the sponsors of the project: GALP Energia, Linde AG Engineering Division, Petronas, Petrobras, Equinor, TOTAL.

References

[1] R. K. Pachauri et L. A. Meyer, Changements climatiques 2014: rapport de synthèse : contribution des Groupes de travail I, II et III au cinquième Rapport d'évaluation du Groupe d'experts intergouvernemental sur l'évolution du climat. Genève (Suisse): GIEC, 2014.
[2] IEA, « CO_2 Emissions Form fuel Combustion », OCDE/IEA, 2018. https://www.iea.org/statistics/co2emissions/ (consulté le 22 juillet 2019).
[3] E. J. Beckman, « Supercritical and near-critical CO_2 in green chemical synthesis and processing », J. Supercrit. Fluids, vol. 28, n° 2‑3, p. 121‑191, 2004.
[4] C Coquelet, P Stringari, M Hajiw, A Gonzalez, L Pereira, M Nazeri, R.Burgass, A. Chapoy., « Transport of CO_2: Presentation of New Thermophysical Property Measurements and Phase Diagrams », Energy Procedia, vol. 114, p. 6844‑6859, juill. 2017, doi: 10.1016/j.egypro.2017.03.1822.
[5] A. Chapoy, M. Nazeri, M. Kapateh, R. Burgass, C. Coquelet, et B. Tohidi, « Effect of impurities on thermophysical properties and phase behaviour of a CO_2-rich system in CCS », Int. J. Greenh. Gas Control, vol. 19, p. 92‑100, nov. 2013, doi: 10.1016/j.ijggc.2013.08.019.
[6] S. Camy, J.-J. Letourneau, et J.-S. Condoret, « Experimental study of high pressure phase equilibrium of (CO_2+NO_2/N_2O_4) mixtures », J. Chem. Thermodyn., vol. 43, n° 12, p. 1954‑1960, déc. 2011, doi: 10.1016/j.jct.2011.07.007.
[7] ISO/TR 27921, « Carbon dioxide capture, transportation, and geological storage — Cross Cutting Issues — CO_2 stream composition », 2020.
[8] M. W. Chase, C. A. Davies, J. R. Downey, D. J. Frurip, R. A. McDonald, et A. N. Syverud, « NIST-JANAF Thermochemical Tables NO_2 ». Standard Reference Data Program National Institute of Standards and Technology Gaithersburg, MD 20899, 1964. [En ligne]. Disponible sur: https://janaf.nist.gov/tables/N-007.html
[9] M. W. Chase, C. A. Davies, J. R. Downey, D. J. Frurip, R. A. McDonald, et A. N. Syverud, « NIST-JANAF Thermochemical Tables N_2O_4 ». Standard Reference Data Program National Institute of Standards and Technology Gaithersburg, MD 20899, 1964. [En ligne]. Disponible sur: https://janaf.nist.gov/tables/N-032.html
[10] K. Yoshino, J. R. Esmond, et W. H. Parkinson, « High-resolution absorption cross section measurements of NO2 in the UV and visible region », Chem. Phys., vol. 221, n° 1, p. 169‑174, août 1997, doi: 10.1016/S0301-0104(97)00149-3.
[11] B. N. Srivastava et A. K. Barua, « Thermal Conductivity and Equilibrium Constant of the System $N_2O_4 \rightleftharpoons 2NO_2$ », J. Chem. Phys., vol. 35, n° 1, p. 329‑334, juill. 1961, doi: 10.1063/1.1731910.
[12] D. R. Powell et E. T. Adams, « Self-association of gases. 1. Theory. Application to the nitrogen dioxide-dinitrogen tetraoxide system », J. Phys. Chem., vol. 82, n° 17, p. 1947‑1952, 1978, doi: 10.1021/j100506a019.
[13] A. J. Vosper, « Dissociation of dinitrogen tetroxide in the gas phase », J. Chem. Soc. Inorg. Phys. Theor., p. 625‑627, 1970, doi: 10.1039/j19700000625.
[14] D. Hurtmans, M. Herman, J. Vander Auwera, « Integrated band intensities in N_2O_4 in the infrared range », J. Quant. Spectrosc. Radiat. Transf., vol. 50, n° 6, p. 595‑602, déc. 1993, doi: 10.1016/0022-4073(93)90027-F.
[15] P. Pascal et P. Baud, Traité de chimie minérale, vol. 1. Masson et cie, 1931.
[16] P. Pascal, « Azote, Phosphore, Arsenic, Industries de l'Azote », in Nouveau Traité de Chimie minérale Tome X, 1958, p. 364‑391.
[17] Z. Yang, « The effect of pressure on the equilibrium of the N_2O_4-NO_2 system, and its classroom demonstration », J. Chem. Educ., vol. 70, n° 2, p. 94, 1993.
[18] R. Schaffert, « The Infrared Absorption Spectra of NO_2 and N_2O_4 », J. Chem. Phys., vol. 1, n° 7, p. 507‑511, juill. 1933, doi: 10.1063/1.1749324.

[19] D. B. Robinson et D.-Y. Peng, The characterization of the heptanes and heavier fractions for the GPA Peng-Robinson programs. Gas processors association, 1978.
[20] C. Coquelet, A. Valtz, et P. Théveneau, « Experimental Determination of Thermophysical Properties of Working Fluids for ORC Applications », in Organic Rankine Cycles for Waste Heat Recovery-Analysis and Applications, IntechOpen, 2019.
[21] P. M. Mathias et T. W. Copeman, « Extension of the Peng-Robinson equation of state to complex mixtures: evaluation of the various forms of the local composition concept », Fluid Phase Equilibria, vol. 13, p. 91‑ 108, 1983.
[22] F. E. C. Scheffer et J. P. Treub, « Determinations of the vapour tension of nitrogen tetroxide », in KNAW, Proceedings, 1912, vol. 15, p. 166‑ 178.
[23] A. C. G. Egerton, « LXVI.—A study of the vapour pressure of nitrogen peroxide », J. Chem. Soc. Trans., vol. 105, n° 0, p. 647‑ 657, janv. 1914, doi: 10.1039/CT9140500647.
[24] J. W. Smith, « CXXVII.—The vapour pressure of intensively dried nitrogen tetroxide », J. Chem. Soc. Resumed, n° 0, p. 867‑ 874, janv. 1927, doi: 10.1039/JR9270000867.
[25] W. F. Giauque et J. D. Kemp, « The Entropies of Nitrogen Tetroxide and Nitrogen Dioxide. The Heat Capacity from 15°K to the Boiling Point. The Heat of Vaporization and Vapor Pressure. The Equilibria $N_2O_4=2NO_2=2NO+O_2$ », J. Chem. Phys., vol. 6, n° 1, p. 40‑ 52, janv. 1938, doi: 10.1063/1.1750122.
[26] G. Baume et M. Robert, « N. Sur quelques propriétés de l'anhydride nitreux pur ou en solution dans le peroxxde d'azote », Comptes Rendus Académie Sci., vol. 169, p. 968, 1919.
[27] A. Mittasch, E. Kuss, et H. Schlueter, « Dichten und Dampfdrucke von wäßrigen Ammoniaklösungen und von flüssigem Stickstofftetroxyd für das Temperatur-gebiet 0° bis 60° », Z. Für Anorg. Allg. Chem., vol. 159, n° 1, p. 1‑ 36, 1927, doi: 10.1002/zaac.19261590102.
[28] V. Tsymarnyi, « Experimental investigation of the P-V-T dependence of nitrogen tetroxide(P-V-T dependence of mixture formed by thermal dissociation of nitrogen tetroxide) », Teplofiz. Vysok. Temp., vol. 5, p. 541‑ 543, 1967.
[29] E. M. Stoddart, « 114. The effect of drying on the vapour pressure of dinitrogen tetroxide and the vapour density of dinitrogen trioxide », J. Chem. Soc., p. 448‑ 451, 1945.
[30] F. E. C. Scheffer et J. P. Treub, « Die Dampfdruckkurve des Stickstofftetroxyds », Z. Für Phys. Chem., vol. 81, n° 1, p. 308‑ 332, 1913.
[31] J. M. Prausnitz, R. N. Lichtenthaler, et E. G. De Azevedo, Molecular thermodynamics of fluid-phase equilibria. Pearson Education, 1998.
[32] A. Belkadi, F. Llovell, V. Gerbaud, et L. F. Vega, « Modeling the vapor-liquid equilibrium and association of nitrogen dioxide/dinitrogen tetroxide and its mixtures with carbon dioxide », Fluid Phase Equilibria, vol. 266, n° 1‑ 2, p. 154‑ 163, 2008, doi: 10.1016/j.fluid.2008.01.026.
[33] A. Anderko, « A simple equation of state incorporating association », Fluid Phase Equilibria, vol. 45, n° 1, p. 39‑ 67, mars 1989, doi: 10.1016/0378-3812(89)80166-9.